

# MODELLING FOR CLIMATE VARIABILITY

---

## Moist Feedback in Large-scale Tropical Circulation

Earlier studies (CM2; CM3; C-MMACS Annual Report 1993-94) have shown that moist feedbacks play a significant role in the genesis and structure of intra-seasonal oscillations in the tropics. These studies were made in an analytical setting, with fixed and separable zonal and temporal structures of the field variables. Other possible roles of moist feedbacks in tropical circulation have been investigated by examining the evolution of tropical circulation as an initial-boundary value problem using a numerical model developed at C-MMACS. It uses a first baroclinic mode vertical structure on an equatorial  $\beta$ -plane and parameterization of two moist feedbacks, namely, evaporation-wind feedback (EWF) and convergence feedback (CF), similar to the analytical model. After validating the model by using initial conditions of a known structure, it was used to investigate two major aspects of tropical circulation described below.

### Role of Moist Feedbacks in organization of the Tropical Flow

One of the outstanding problems in numerical modelling and prediction of atmospheric flow is that of climate drift. Small errors present in the initial field and cumulative numerical error can cause the model-simulated field to drift away from the observed climatology. While the exact mechanism for this climate drift is

not known, it is believed that nonlinear interactions play a key role. In order to investigate and identify any physical process that may contribute to this problem, extensive numerical experiments have been carried out with the numerical model.

These experiments were designed to investigate the evolution and the structure of an initial random field of small amplitude in the presence of moist feedbacks. Thus with initial random fields for zonal velocity  $u$ , meridional velocity  $v$ , and potential temperature  $\theta$ , the model was integrated for time durations determined by predictability studies. The results for a typical run are shown in Fig. 2 for a moderate value of the strength of CF and three values of EWF. The three panels show longitude-latitude structure of the model  $u$ -field after 150 days of model integration. It is seen from these panels that when EWF is zero, a random initial field remains random even after 150 days. In the presence of EWF, however, the random field gets organized into a structure which is periodic in East-West direction and trapped in the North-South direction, and is also periodic in time (Fig. 3). Also it can be seen from these figures that the model fields closely resemble a Kelvin wave. The structure of the model velocity field is also found to be rather insensitive to the strength of moist feedbacks. It is accordingly proposed that an initially random field and its subsequent development as shown in this study can contribute to the climate drift in models of tropical circulation.

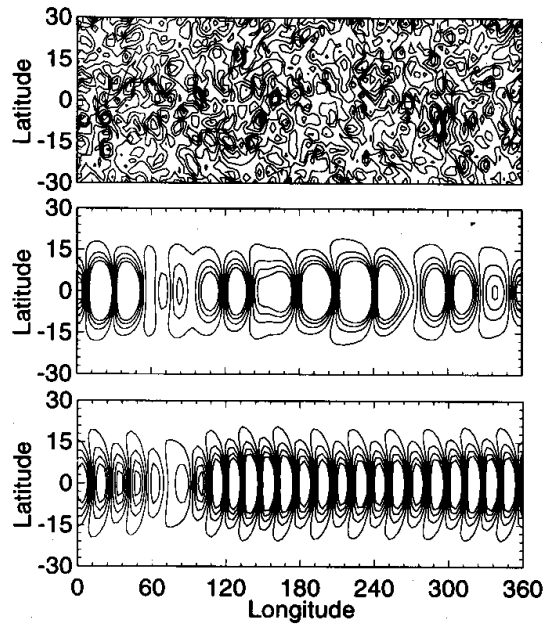


Figure 2: Longitude – latitude structure of the model  $u$ -field after 150 days of model integration, starting from a random initial field for a moderate value of Convergence Feedback (CF) and different strengths of Evaporation Wind Feedback (EWF): Top panel: Zero EWF; Middle Panel: Weak EWF; Bottom panel: Strong EWF.

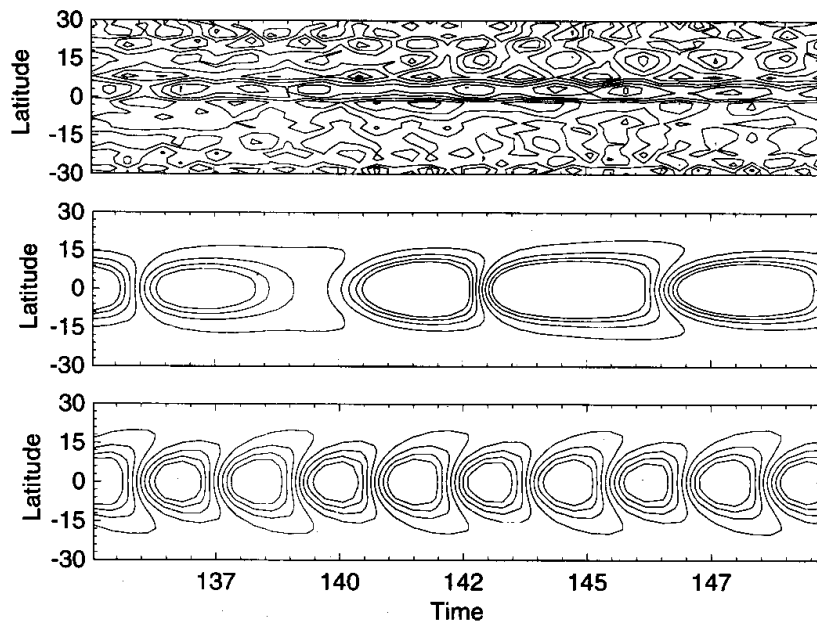


Figure 3: Time – latitude structure (from 135th day to 150th day) of the  $u$ -field (at  $180^\circ$  E), starting from a random initial field for a moderate value of CF and different strengths of EWF: Top panel: Zero EWF; Middle panel: Weak EWF; Bottom panel: Strong EWF.

### **Effect of Land-Ocean Contrast on Tropical Circulation**

Many parts of the tropics, especially in the Indian Ocean region, are characterized by the presence of land. The presence of these land masses introduce inhomogeneities in the lower boundary forcing of the atmosphere and thus can significantly affect the structure and evolution of the tropical circulation. The inhomogeneity of atmospheric forcing associated with land-ocean contrast (LOC) can also affect the predictability of the tropical flows. Results of numerical experiments with the model incorporating two simple LOC parameterizations supported the above hypotheses. (*P Goswami and B Joseph*)

### **Hybrid Prediction System Based on Neural Network and Dynamical Model**

An outstanding problem in operational forecasting of complex dynamical systems such as the atmosphere and the ocean is the limited range of predictability due to growth of error during numerical integration. At present, numerical integration of such dynamical models provide the only method of operational forecasting of oceanic and atmospheric flows. In recent years, another modelling technique, known as artificial neural network (NN) has gained popularity. While a dynamical model predicts the future trajectory of an initial point, NN is used to model an input-output mapping of a given set of points, which is generally an observed data set. Unlike a dynamical model, which has the advantage of being based on well understood formulations of relevant physical processes, the NN methodology does not explicitly incorporate such knowledge. A paradigm of hybrid prediction is being developed at C-MMACS under a project sponsored by the Department of Science and

Technology (DST) to combine the advantages of both the methodologies. The proposed methodology consists of training an NN of suitable configuration on data generated by short-term integration of the numerical model. The trained NN is then used to make short range prediction of the process. The NN prediction is then used to correct and modify subsequent prediction of numerical integration. This procedure, carried out iteratively, helps to suppress the error developing in numerical integration, thereby increasing the range of prediction. Although the ultimate goal is to develop such a methodology for improving medium range weather forecasting, the present phase was devoted to development and evaluation of the methodology for a considerably simpler test system. A Duffing oscillator, which exhibits both chaotic and non-chaotic behaviour depending on the parameter range, was chosen as the test system as it seems to be an appropriate nonlinear system in view of the known nonlinear features of oceanic and atmospheric processes. A methodology was adopted to evaluate the acceptability of a hybrid configuration, based on a hierarchy of criteria. These criteria ensured that global energetics as well as other global characteristics of the dynamical system are preserved by the hybrid model. Acceptability of four hybrid configurations (HM1-HM4) based on these criteria is shown for four initial conditions (NMC1-NMC4) in Table I for two periods of integrations, 350 cycles and 250 cycles. After a hybrid configuration was accepted on the basis of the acceptability criteria, its performance was judged according to a set of performance criteria. The two major performance criteria adopted are as follows:

1. The difference between the simulations from the numerical model and the hybrid model should be less than or comparable to the natural variability (measured by variance) of the numerical model simulation.

Group (Initial Conditions)	Simulation	Statistical Characteristics								Best Performance	
		Run1 (Upto 200 cycle)				Run2 (Upto 350 cycles)				Run1	Run2
		Min	Max	Amp	Mean	Min	Max	Amp	Mean		
A $Y(0)=1.0$ $Y'(0)=0.0$	DM1	-1.41	1.35	1.38	-0.47	-1.49	1.43	1.46	-0.09	HM2	HM2
	HM1	-1.38	0.00	0.69	-0.79	-1.51	1.44	1.47	-0.64		
	HM2	-1.51	1.41	1.46	-0.24	-1.51	1.51	1.51	-0.28		
	HM3	-1.34	0.00	0.67	-0.81	-1.34	0.00	0.67	-0.82		
	HM4	-1.37	0.00	0.68	-0.82	-1.36	0.00	0.68	-0.82		
B $Y(0)=1.05$ $Y'(0)=0.0$	DM2	-1.47	1.42	1.45	0.27	-1.47	1.42	1.42	0.25	HM1	HM1
	HM1	-1.52	1.42	1.47	0.59	-1.52	1.51	1.51	0.56		
	HM2	-1.44	1.50	1.47	-0.36	-1.44	1.50	1.47	-0.53		
	HM3	-1.52	1.52	1.52	-0.21	-1.52	1.52	1.52	-0.04		
	HM4	-1.47	1.49	1.48	-0.45	-1.47	1.49	1.48	-0.62		
C $Y(0) = 1.10$ $Y'(0) = 0.0$	DM3	-1.47	1.51	1.49	-0.32	-1.47	1.51	1.49	-0.53	HM2	HM1
	HM1	-1.50	1.40	1.45	-0.62	-1.50	1.40	1.45	-0.61		
	HM2	-1.51	1.49	1.50	-0.52	-1.51	1.49	1.50	0.04		
	HM3	-1.36	0.00	0.68	-0.82	-1.36	0.00	0.68	-0.82		
	HM4	-1.35	0.00	0.68	-0.82	-1.35	0.00	0.68	-0.82		
D $Y(0) = 1.15$ $Y'(0) = 0.0$	DM4	-1.43	1.51	1.47	-0.09	-1.43	1.51	1.47	-0.14	HM2	HM2
	HM1	-1.49	1.49	1.49	0.35	-1.49	1.49	1.49	0.44		
	HM2	-1.39	1.41	1.40	-0.28	-1.49	1.41	1.45	-0.38		
	HM3	-1.38	1.35	1.36	0.00	-1.38	1.35	1.36	-0.34		
	HM4	-1.36	1.27	1.32	-0.71	-1.36	1.27	1.32	-0.76		

Table 1: Comparison of statistical properties of the numerical model simulation of four versions of the dynamical model DM1 - DM4 for trajectory  $y(t)$  with those of four versions of the hybrid model HM1 - HM4. Comparisons are also drawn for the evolution from four groups of initial values (A-D) as indicated.

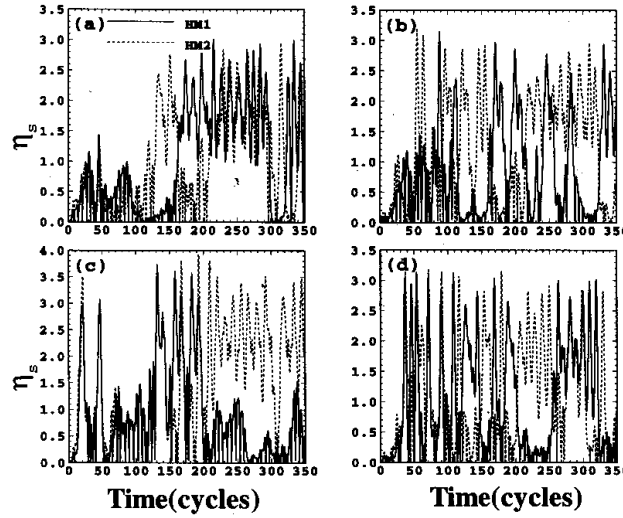


Figure 4: Time evolution of simulation index  $\eta_s$  for two versions of hybrid model HM1 (dashed line) and HM2 (dotted line).

2. The signal-to-noise ratio for the hybrid model should be less than the corresponding value for the numerical model.

Fig 4 and 5 represent the performance of two accepted hybrid configurations (HM1 and HM2) according to the two performance criteria. Fig 4 represents the ratio of the difference of the two simulations to the standard deviation  $\eta_s$  of the numerical model simulation as a function of time for two hybrid configurations (HM1 and HM2). The four panels (a) through (d) correspond to the four initial values of  $y_0$ , i.e. 1.0, 1.05, 1.1 and 1.15 respectively. The initial value of the momentum variable  $y'$  has been kept constant at 0 for all the experiments. The plots have been smoothened by taking 10 cycle running average. In Fig. 5 the signal-to-noise ratio for three configurations: numerical model, HM1 and HM2 are shown for three values of perturbation: 5 % (panel a), 10 % (panel b) and 15 % (panel c) of the initial amplitude  $y_0 = 1.0$ . The momentum variable  $y'$  was given the same initial value in all the three experi-

ments. The curves are smoothened with 100 points (10 cycles) running average. The overall performance of HM2 in noise suppression is seen to be better than the numerical model. The present phase of this work focusses on developing and testing the paradigm and the methodology. The work is now in progress on more complicated coupled nonlinear dynamical systems. (*P Goswami, S Sarangi and P Bhoominathan*)

## Sea Level Change

In an earlier work (C-MMACS Annual Report 1993-94), fractal dimension of sea level data was found to be in the range 1.2 to 1.3 for five stations on the Indian coast. The same method, that is, iterative functions system (IFS) technique was applied during the reporting period to the remaining four Indian stations for which long time series data were available, and it was found that the range remains unaltered. Interestingly, when this technique

was applied to four stations on the coast of China, the results were in the same range. It is concluded that sea level variation in Indian and Pacific Oceans can be modelled as a dynamical system with a few degrees of freedom. (N K Indira; R N Singh\*, \* NGRI)

## Basin Scale Ocean Modelling

Large scale circulation in ocean is known to influence climate, availability of living marine resources, and navigation. Since observations in oceans tend to be sparse and very expensive, modelling has emerged as a powerful tool for investigating several features of ocean circulation. Large scale circulation in Indian Ocean has been studied in a project sponsored by the Department of Ocean Development (DOD) by simulating the world ocean with the use of the Modular Ocean Model (MOM). This model has been developed by the Geophysical Fluid Dynamics Laboratory (GFDL), Princeton University, over two decades and is extensively used on account of its versatility. The present simulation uses a grid of nearly 1 million points ( $1^\circ \times 1^\circ$ , and 15 vertical levels) and a computational time step of 1 hour. Integration is carried out for a total of 75 years with climatological surface winds. Also, computed temperature and salinity in the first 1000 metres of the ocean seem to compare well with observations. The climatological run is used as the basic case for studying the effects of perturbations due to a variety of forcing fields. Results obtained after integration for 75 years are given in Fig. 6 for four seasons. They are intended to show how surface ocean currents vary seasonally in a typical year. One notices a strong westward north equatorial current in January and associated counter current eastward in the southern ocean. In April, the former has weakened and the latter has shifted closer to the equator. The surface currents in July are very intense off the Somali coast in response to strong mon-

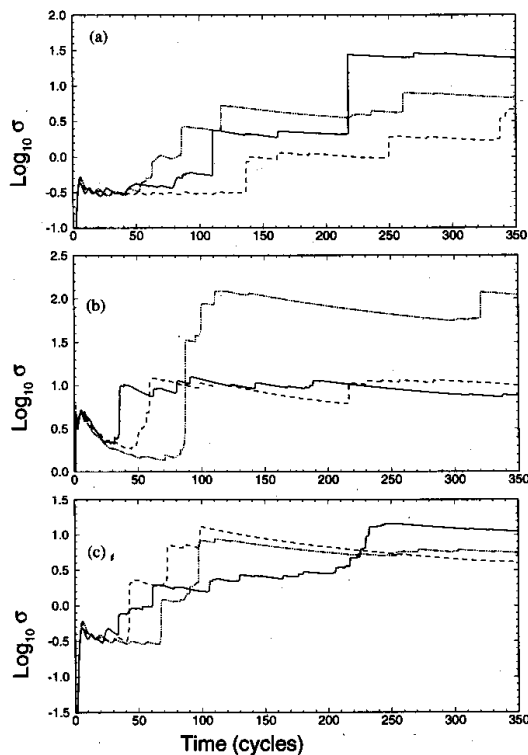


Figure 5: Signal to noise ratio ( $\sigma$ ) as a function of time for DM (solid line), HM1 (big dash line) and HM2 (small dash line) simulations.

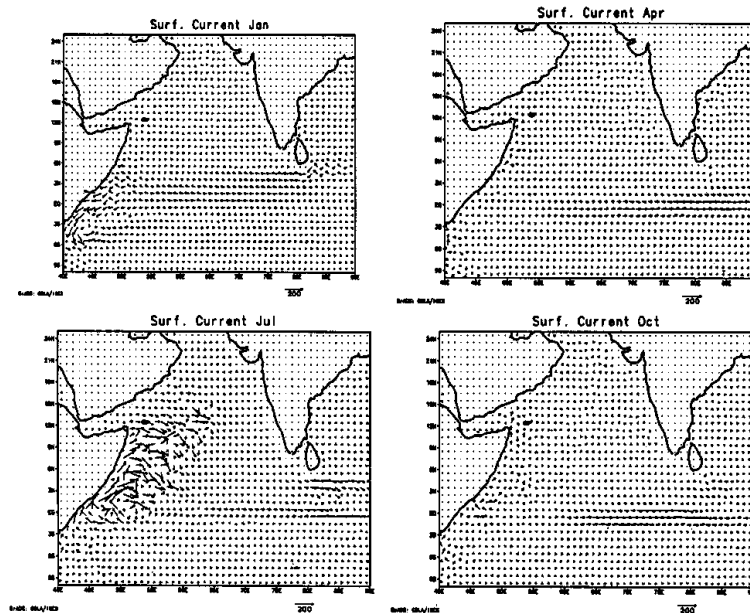


Figure 6: Seasonal variation of surface circulation in the Indian Ocean Basin: Results of simulation after 75 years of integration of the Modular Ocean Model (MOM).

soon winds with the characteristic Findlater jet. The currents in October show reduced intensities near Somali coast and intensification of the equatorial counter current. One also notices in Fig. 7 that currents off the east coast of south India are northward in some seasons and southward in others, which are largely due to seasonal change in wind direction over the Bay of Bengal. These simulations are consistent with well known climatological features. (*P S Swathi, K S Yajnik*)

### **Air-Sea Interaction and Coupled Intra seasonal Oscillation**

The important role played by air-sea interaction in the genesis and dynamics of inter-annual variabilities in the tropics notably the El-Nino and the Southern Oscillation (ENSO) has long been known. Recent observational and modelling studies, however, show that air-

sea interaction plays a crucial role even at intra seasonal time scales. Studies were carried out to identify proper modelling of air-sea interaction which can support intra-seasonal oscillations in a coupled environment. It was found that the presence of moist feedbacks can generate and destabilise new modes at intraseasonal frequencies that would be absent in an uncoupled environment. For coupled equatorial Kelvin waves, the coupled system can support two unstable eastward propagating branches, one with a maximally growing wave with a period of about 30 days and the other with a period around 60 days. The characteristics of these waves are very similar to those of the 30-60 day intraseasonal oscillation observed in the tropics. Thus the present formalism offers a natural explanation of the quasi-periodicity (30-60 days) of the major observed intraseasonal oscillation in the trop-

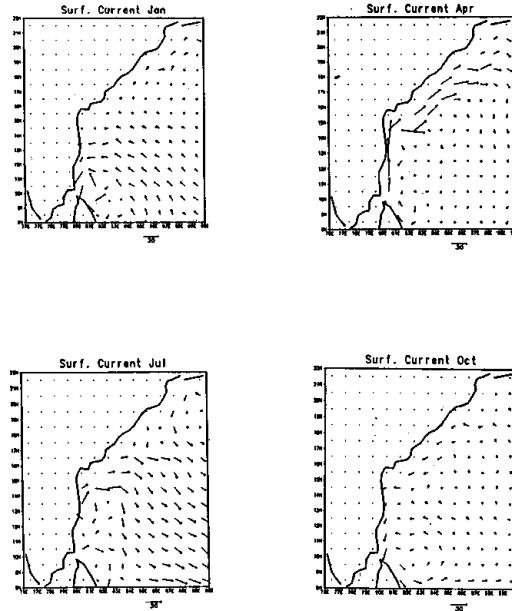


Figure 7: Seasonal variation of surface circulation off the east coast of India: Results of simulation after 75 years of integration of MOM

ics. In addition, the present formalism offers a number of necessary conditions for the existence of coupled instability. Analysis of the dispersion relation for a standard set of parameters shows that there are three maximally growing waves in the two branches of the solution. One of these maximally growing waves corresponds to a time period of 60 days and a wavelength of about 12,000 km. The other two maximally growing waves have time periods between 20 - 30 days and wavelengths between 20,000 - 30,000 km. The present results have been obtained with linearised equations on an equatorial  $\beta$ -plane, with a first baroclinic mode vertical structure. Since air-sea interaction, on which the emphasis has been laid in the present studies, plays a crucial role in performance of coupled models, these studies can make significant contribution to the formulation and the validation of ocean-atmosphere coupled mod-

els for the tropical climate. Studies are now being carried out to investigate the implications of this parameterization scheme in more complex nonlinear situations. (*P Goswami, K Rameshan*)

### Modelling of Inter-annual Variability in the Indian Ocean

The existence of a coupled ocean - atmosphere oscillation in the tropics, known as El-Nino Southern Oscillation (ENSO) has been known for a long time. Recent more detailed observational analysis of observations has shown that contrary to earlier belief, the ENSO phenomenon is more global in character and warm episodes almost in phase with El-Nino events in the western pacific appear also in the Indian ocean. These warm episodes are however of much smaller amplitudes (0.5 degree C) compared to those over the Pacific region ( $\approx 2$



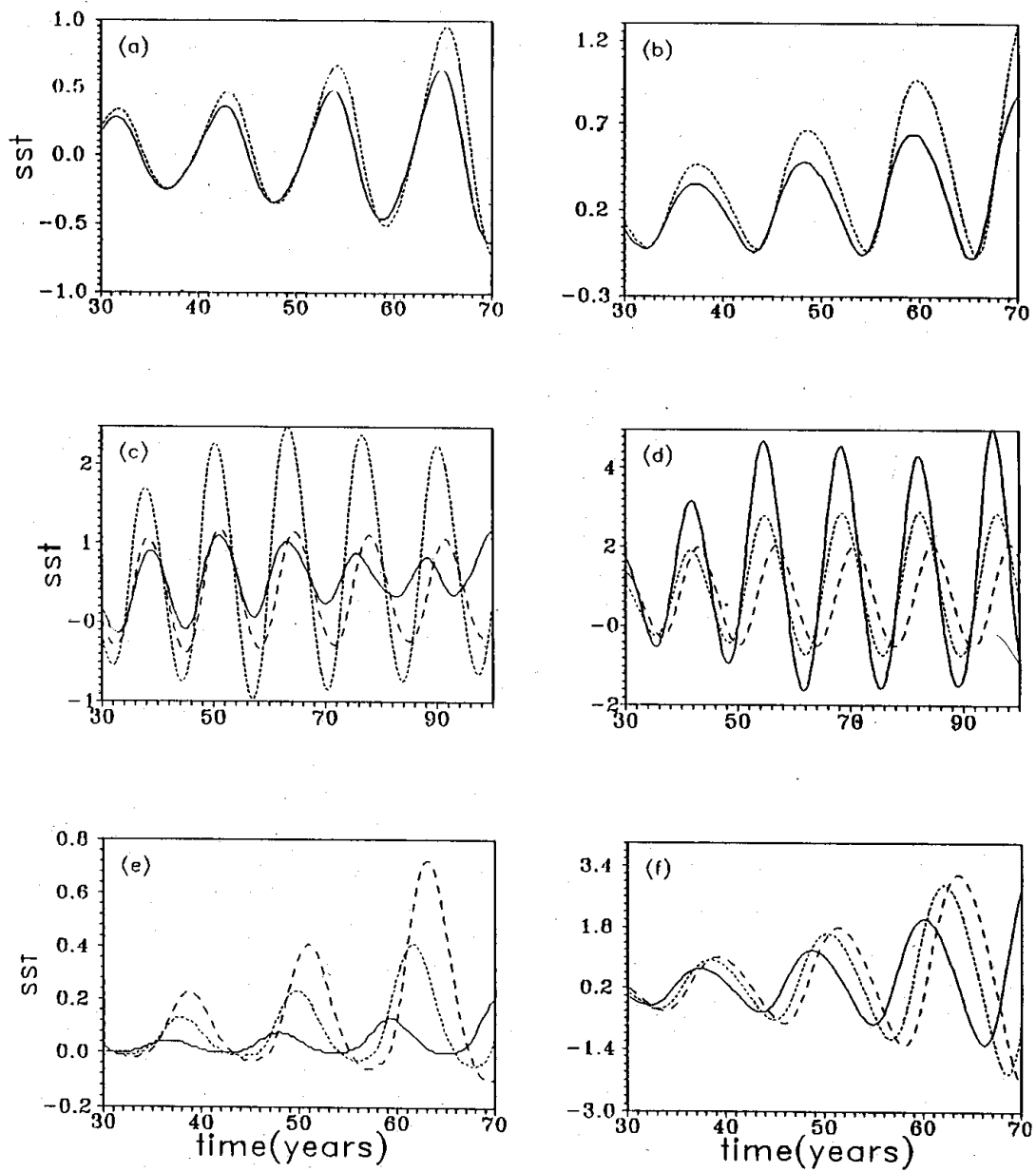


Figure 8: Time series of basin averaged sea surface temperature field. Top panels: only ocean; Middle panels: equal ocean; Bottom panels: for unequal ocean basins. (a), (c), (e) refer to western basin and (b),(d) & (f) refer to eastern basin. Solid line: no EWF; Small dash line: moderate EWF; Big-dash line: high EWF

degree C). In the conventional dynamical scenario for ENSO, only large basins of the size of the Pacific can support ENSO-type oceanic variability. It appears therefore that some other mechanism or some other aspect of air-sea interaction must be considered to account for the complete set of interannual variabilities. Using a simple two-dimensional model, Anderson and McCreary (AM) showed that inclusion of basin configuration (an 'Indian' ocean separated from a larger 'Pacific' basin by a strip of land) plays an important role in determining the structure of the interannual variabilities over the two basins. However, the small basin exhibits a stable (weakly warm) state while the larger basin exhibits interannual variabilities. To understand the mechanisms of weak interannual variability over the Indian ocean, a minimal 'coupled' model was developed at C-MMACS as a part of a project supported by the DOD (CM 23). The model has a "minimal" dynamics (one-dimensional, zonal motion) and the emphasis is on air-sea interaction. It was found that even in the one-dimensional case, the basic nature of the variabilities over the two basins is similar to those found in the two-dimensional model of Anderson and McCreary. However, a new feature is brought about by inclusion of moist feedback, viz evaporation-wind feedback, not present in AM. Fig. 8 shows the time series of basin averaged SST field for three cases: The top panels show the time evolution of SST for an all ocean case while the middle panels show the time evolution of SST for the two equal ocean basins separated by a strip of land. The bottom panels show the results for the unequal ocean basin case. As can be seen from this figure (the bottom panels), presence of EWF brings about an oscillation in the smaller ocean basin, with amplitude about  $0.5^{\circ}$  C. In contrast, the presence of EWF has no significant effect over the amplitude of the variabilities over the larger basin.

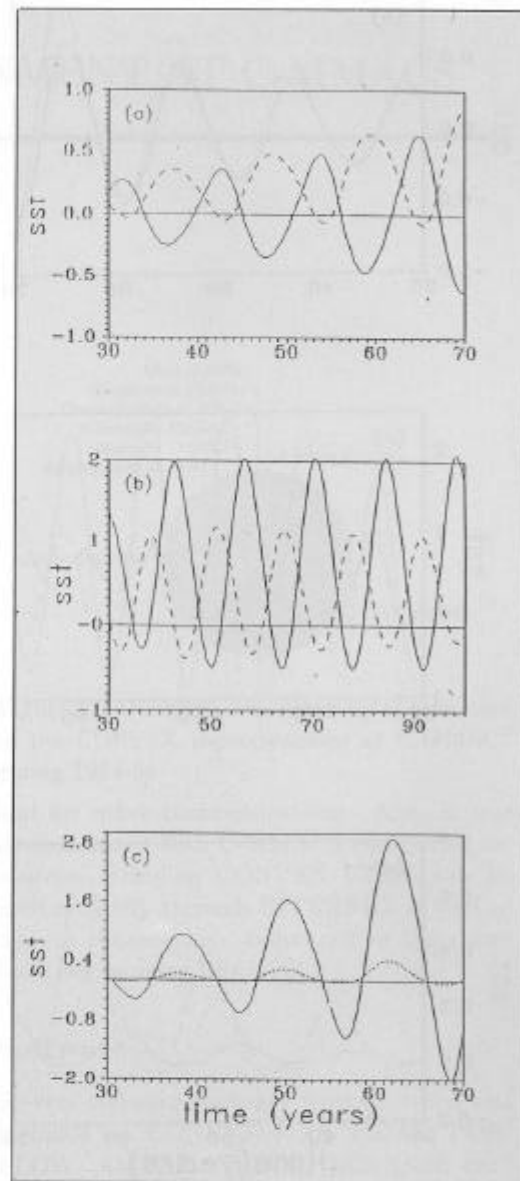


Figure 9: Phase relationship between the two basin averaged SSTs for (a) the all ocean case, (b) the equal ocean basin case. Dashed line represents basin 1 and the solid line represents basin 2.

An interesting prediction of the present model is that the 'Indian' ocean variabilities are always warm episodes (Fig. 9). They do not exhibit the cold 'La-Nina' state seen for variabilities over the Pacific. Analysis of model

fields revealed that basin geometry mainly affects oceanic downwelling while EWF affects the atmospheric heating field. Investigation of these processes with more complex models is currently under progress. (*P Goswami, H Nandini*)